Polypropylene and Polyethylene−Copolymer Blend Miscibility: Slow Chain Dynamics in Individual Blend Components near the Glass Transition

Marcin Wachowicz, Lance Gill, Justyna Wolak,† and Jeffery L. White*

Department of Chemistry, Oklahoma State University, Stillwater, Oklahoma 74078

Received December 15, 2007; Revised Manuscript Received January 29, 2008

ABSTRACT: We systematically evaluate the slow conformational reorientations of polypropylene (PP) and polyethylene-*co*-1-butene (PEB) chains at temperatures near T_g before and after formation of a miscible blend with chain specific experiments. Solid-state ^{13}C CODEX and static ^{129}Xe NMR experiments reveal that aPP and PEB66 (PEB copolymer with 66 wt % 1-butene) are intimately mixed at the chain level. The two pure polymers, differing in T_g by ca. 50 K, exhibit large differences in the central correlation time constant τ_c for slow chain segmental motion (1–1000 ms) at any temperature but have equal correlation time distributions at/near T_g. In the miscible blend, slow chain dynamics are characterized by essentially equal central correlation time constants τ_c (ca. 15 ms) at a common temperature corresponding to the maximum exchange intensity for segmental rearrangement in the CODEX experiment, but the widths of the correlation time distributions diverge dramatically at any temperature, including at/near T_g. On the basis of comparisons of quantitative Arrhenius vs WLF models, and using an Adams−Gibbs treatment of the data, we determine that the overall configurational entropy S_c in the aPP/PEB66 blend exceeds that of the unmixed components by 15%, in agreement with previous work (*Macromolecules* **2007**, *40*, 5433). On the basis of the experimental data, general conclusions regarding driving forces for polyolefin miscibility and slow chain dynamics in miscible blends are discussed in the context of recent proposals in the literature, recognizing that polyolefins represent a limiting case of macromolecular thermodynamics due to their nonpolar structure. Importantly, all data are measured on individual signals from each polymer component in the solid blend.

Introduction

Several key questions relevant to the design, synthesis, and application of heterogeneous polymer materials can be addressed experimentally using binary blends of polyolefins. Although polyolefins are the most chemically "simple" polymers, the complexities of phase behavior over an almost endless array of economically important blend, copolymer, and nanocomposite applications is reflected in the lack of understanding about miscibility in simple binary mixtures of polyolefins.[1–5] Stated simply, one cannot predict a priori whether two synthetic polyolefins will form a miscible mixture and, therefore from a mechanical properties perspective, a new material. Recently, several groups including our own have investigated these questions using polyolefin blends as a limiting class of macromolecules in which specific chemical interactions are minimized due to their completely saturated sp^3 carbon structure.[6–11] Chain organization and dynamics control the observed mechanical properties, and while many polyolefin blends are semicrystalline, important limits on phase behavior can be established by examination of amorphous blends. From a practical perspective, new materials are often desired with properties intermediate between the two constituent polymers, which is often characterized by the difference in their glass transition temperatures T_g. There has been considerable attention in the literature regarding mechanically relevant chain dynamics in amorphous polymers and their blends (with component polymers exhibiting large T_g differences), although, in many cases, at temperatures well above T_g. Specifically, the relative contributions of self-concentration (i.e., intrachain) and concentration fluctuation effects to segmental dynamics in pure and mixed polymers, as well as their effects on the cooperative rearrangements near T_g, have been discussed.[12–20] Key differences in these models lie in the details regarding temperature dependence of characteristic segmental relaxation lengths, length scales for the glass transition, and intrachain vs interchain contributions.

In a recent paper, we have shown by direct chain measurement solid-state NMR experiments that the polyolefin blend PIB/hhPP (polyisobutylene/head-to-head polypropylene) is intimately mixed at the chain level, that the mixing is driven by increased configurational entropy in the blend, and that individual slow segmental chain dynamics (1 ms $< \tau_c <$ 1000 ms) near T_g respond in a nonlinear fashion upon mixing and are characterized by unique changes in correlation time distributions.[21] In this contribution, we have examined more commercially relevant blend systems involving atactic polypropylene (aPP) and polyethylene−1-butene copolymers (PEB) containing differing amounts of butene comonomer. Our model-free experimental observations based on a similar direct/selective chain-measurement strategy are that aPP is intimately mixed with PEB containing 66 wt % 1-butene comonomer, and at or near T_g, slow segmental dynamics become even more heterogeneous in the miscible blend than in the pure polymers, particularly for the high-T_g aPP component. The experiments spanned the full range of temperatures for each pure component glass transition and that of the blend. Through comparative application of Arrhenius/log-Gaussian vs WLF/KWW models for analysis of the temperature-dependent CODEX[22,23] exchange intensities, we determine that in the miscible aPP/PEB-66 blend the central correlation time constants τ_c converge to essentially identical values at a common intermediate temperature relative to the unmixed components, but that the correlation time distributions widths diverge from one another in the blend and from their pure component values. This is particularly evident for the high-T_g aPP component, which exhibits a ca. 3 decade increase in

* To whom all correspondence should be addressed. E-mail: jeff.white@okstate.edu.

† Present address: Department of Biomedical Engineering, University of North Carolina, Chapel Hill, NC.

10.1021/ma702795b CCC: $40.75
Published on Web 03/13/2008

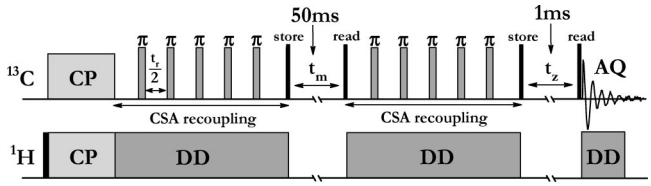

Figure 1. CODEX experiment pulse sequence applied under conditions of MAS. The value of the exchange mixing time $t_m = 50$ ms for all aPP, PEB, and blend data reported in this paper. The total CSA evolution time corresponding to the sum of the first and second recoupling period $2(3t_r) = 1.5$ ms.

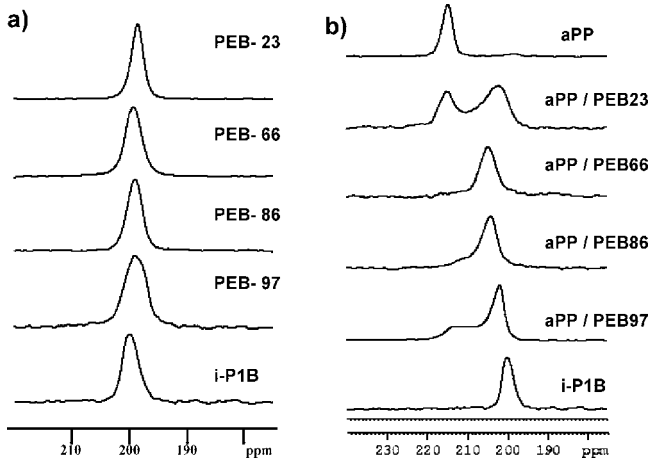

Figure 2. ^{129}Xe static NMR results for xenon gas absorbed in (a) a series of pure PEB-*xx* copolymers, with *xx* indicating the weight percent of 1-butene content, and (b) the blend of aPP with the same PEB copolymers. Pure isotactic poly-1-butene is denoted i-P1B. Details of the Xe NMR experimental conditions may be found in ref 31.

its correlation time distribution in the blend relative to its pure state, far exceeding the ca. 1 decade increase for the low-T_g PEB66 component in the blend. The pure polymers themselves are characterized by 1–2 decade wide correlation time distributions near T_g, decreasing as temperature is increased. Quantitative analysis of all of the temperature-dependent correlation time data in the unmixed and blended polymers reveals that the total configurational entropy increases by 15% in the blend relative to the pure polymer components.

Experimental Section

Samples and Data Collection. Atactic polypropylene (aPP) was a commercial sample acquired from Eastman, characterized by a DSC $T_g = -11$ °C and $M_n = 29\,600$. The PEB-66 ($M_w = 114\,000$, $T_g = -54$ °C) is the same polymer previously referenced as HPB66 by Graessley and co-workers and is a monodisperse ethylene−butene copolymer obtained by anionic polymerization of butadiene, followed by hydrogenation.[24] The degree to which the diene polymerizes 1,2 vs 1,4 addition determines the butene and ethylene concentrations, respectively, as has been extensively discussed in previous papers.[24,25] The PEB-23 sample is a commerical ethylene−butene copolymer made via metallocene polymerization ($M_w = 79\,000$) and sold as Exact 4041 by ExxonMobil. Other PEB copolymers mentioned in Figure 2 are a combination of commercial or anionically polymerized materials and are denoted numerically by their percent weight butene comonomer content. The 50:50 wt % blends were prepared from dissolution in toluene for 24–48 h, followed by solvent evaporation, and then vacuum-drying to 10^{-2} Torr for 4 days or longer. The DSC T_g for the blend was −36 °C (5 K/min scan).

All ^{13}C and ^{1}H measurements were collected on a Bruker DSX-300 with field strength equal to 7.05 T. Solid-state CODEX NMR experiments were performed on a 4 mm double-resonance magic-angle spinning probe using the pulse sequence in Figure 1, previously described in detail by Schmidt-Rohr.[22,23] The probe temperature was calibrated using $PbNO_3$ to within ±1 K. All CODEX exchange data were acquired with an actively controlled 4 kHz MAS speed, a 1 ms cross-polarization contact time, and rotor synchronization, and as a precaution, measurements were altered between the CODEX and reference signal every 256 scans to eliminate spectrometer drift. All CODEX slow exchange data were acquired using a 50 ms exchange time, unless otherwise noted. Total experiment times typically ranged between 8 and 12 h for a single measurement, depending on the temperature.

Calculations and Theory. The data analysis methods we use here are the same as those we recently described for a different polyolefin blend system[21] and are described in detail in the Supporting Information. Chain conformational exchange data from variable temperature CODEX experiments were analyzed to extract correlation time constants, activation energies for chain reorientation, and quantitative correlation time distributions. An isotropic rotational diffusion model (employing 20 discrete conformer populations as an approximation to the heterogeneous backbone conformer distribution) was used to simulate the experimental data and solve the overall equilibrium exchange matrix as a function of the exchange mixing time in the CODEX experiment and the correlation time constant for the specific polymer at each temperature. A discrete log-Gaussian correlation time distribution function was analyzed with respect to temperature using an Arrhenius model, which was also compared to results from a WLF/KWW model analysis of the experimental data. Powder averaged values of the chemical shift anisotropy, reflecting the distribution of tensor orientations in the amorphous polymers, were included in all calculated fits of the data. The *Mathematica* program (version 5.2) was used for all calculations. The theory regarding exchange intensities has been previously developed for static samples, and the incorporation of the additional terms arising from the time dependence of the frequency introduced by MAS has also been described.[26,27] Complete details for all calculations as implemented for the pure polymers and their blends are described in ref 21 and in the Supporting Information. For convenience, the equation describing the quantitative evolution of the normalized exchange intensity E as a function of exchange time and temperature for a distribution of correlation times $g(\tau)$ is reproduced here in eq 1:[26]

$$E(t_m, \tau_c, T) = \frac{S_0 - S}{S_0} = \frac{\int_0^\infty \{\mathrm{Re}[G_-(t_z, \tau, T)] - \mathrm{Re}[G_-(t_m, \tau, T)]\} g(\tau)\, d\tau}{\int_0^\infty \mathrm{Re}[G_-(t_z, \tau, T)] g(\tau)\, d\tau} \quad (1)$$

All additional terms are defined and described in the Supporting Information, but the reader can quickly note the time dependencies for the specific delays in the Figure 1 pulse sequence from this equation.

Results and Discussion

Candidates for a Miscible aPP/PEB System. In order to determine whether PP and PE copolymers can form miscible, intimately mixed chain-level blends and, more importantly, understand why they do or do not exhibit such behavior, one must first narrow the field of all possible choices reported in the recent literature.[8,24,28–30] In this investigation, we limit our investigations to amorphous systems, since phase separation in amorphous binary blends typically implies phase separation in their crystalline counterparts. ^{129}Xe NMR diffusion/equilibration experiments can indicate which blends are intimately mixed, albeit with a minimum length scale much longer than constituent radii of gyration, as we previously demonstrated for PIB/PEB blends.[31] In other words, it is a quick and reliable test for

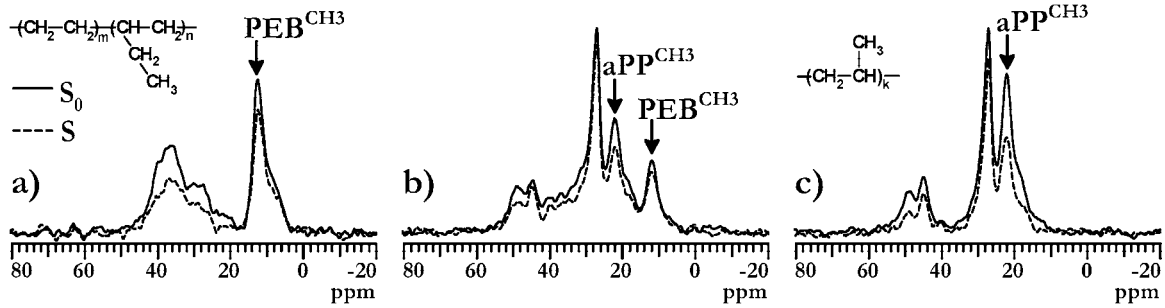

Figure 3. Example ^{13}C CODEX spectra for (a) pure PEB66 at 225 K, (b) aPP/PEB66 50/50 wt % blend at 250 K, and (c) pure aPP at 274 K. Solid line is the reference spectrum S_0, whereas the dashed line corresponds to the spectrum obtained with mixing time = 50 ms (S).

microphase separation for blends, since the observation of distinct peaks for Xe in each polymer component in the blend indicates regions of single-component density whose dimensions exceed that of the Xe diffusion coefficient length scale (ca. ≥35 nm).[31,32] While this is a relatively coarse-grained experimental probe compared to molecular/chain dimensions, it does provide valuable limiting information. Figure 2 shows a series of static ^{129}Xe NMR spectra for several pure PEB copolymers (a) and for blends of aPP with the same PEB copolymers (b).

Figure 2a is a control experiment to verify that the xenon shielding environment is insensitive to comonomer concentration in the PEB copolymer series ranging from 23 to 97 wt % butene comonomer. As shown in Figure 2a, all PEB copolymers, as well as pure isotactic poly-1-butene, exhibit a similar ^{129}Xe chemical shift of 197–198 ppm. In contrast, Figure 2b indicates that the shift for xenon gas in pure aPP is 215 ppm, an expected result given the well-known sensitivity of xenon gas to different polymer densities. Most importantly, the spectra in Figure 2b for blends of aPP with the different PEB copolymers clearly indicate that the only blend where Xe is sampling a homogeneous polymer environment on the time scale defined by its diffusion coefficient (ca. 2×10^{-7} cm^2 s^{-1}) is the blend of aPP with PEB-66; the other three blends show two well-defined peaks consistent with the same peaks observed in the pure polymer components. The center of mass for the aPP/PEB-66 peak is 205 ppm; the expected composition-weighted average for the 50:50 wt % blend is 206 ppm. Of the various PEB copolymers in Figure 2, most of which have been previously discussed as candidates for miscible blends with aPP, Figure 2b indicates that only PEB-66 is a viable possibility. For this reason, detailed investigations of individual chain mixing and dynamics using more advanced and time-consuming CODEX methods will be limited to the aPP/PEB-66 blend in the remainder of this contribution.

Slow Chain Dynamics near T_g in aPP, PEB-66, and aPP/PEB-66 Blend by CODEX NMR. The CODEX experiment is a one-dimensional constant-time version of classic two-dimensional exchange experiments that exploits the anisotropy of the chemical shift interaction to detect movement (in real time) of polymer chain segments.[22] The experiment is run in duplicate to generate two data sets, which differ in that the t_m and t_z periods are interchanged, generating what is known as the exchange spectrum S (t_m and t_z positioned as shown in Figure 1) versus the reference spectrum S_0 (no mixing; t_m and t_z switched from that shown in Figure 1). The pure exchange spectrum is the difference between these two results, denoted as $\Delta S = S_0 - S$. From eq 1, the amplitude of this signal is related to the normalized exchange intensity as $E(t_m,\tau_c,T) = \Delta S/S$. Systematic comparisons of E as a function of temperature for pure polymers versus the same polymers in the binary blend can reveal quantitative changes in slow chain dynamics and their distributions (1–1000 ms correlation time constants) upon blend formation. Figures 5S and 6S in the Supporting Information

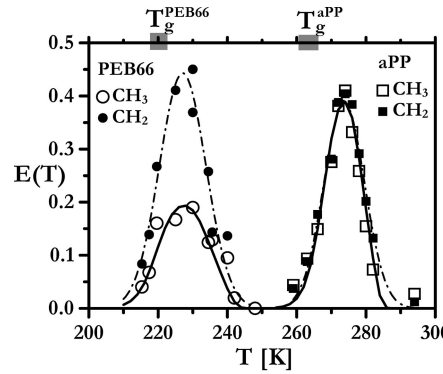

Figure 4. Normalized exchange intensities $E(T)$ for methyl and methylene signals of pure PEB66 and pure aPP. The solid lines are Arrhenius model fits (see below) to methyl data points, whereas the dash-dot lines are drawn through the methylene experimental points only to guide the eye. For reference, the T_g ranges via DSC are shown at the top of the figure.

provide additional details on mixing time and recoupling time dependencies for these polymers.

Figure 3 shows representative results for pure PEB-66, pure aPP, and their blend at temperatures near the maximum exchange intensity for each sample. As discussed previously, when the temperature is low compared to the polymer T_g, no chain motion occurs, and the exchange intensity is zero. The CODEX experiment detects chain dynamics as the polymer proceeds through T_g, with a characteristic exchange frequency window of 1–1000 Hz. At high temperatures, chain reorientation occurs with a correlation exchange frequency greater than that of the chemical shift anisotropy mechanism by which the CODEX sequence detects motion through echo attenuation. If the polymers become too mobile at high temperatures, then the ability to detect chain motion is precluded and the exchange intensity vanishes. For the amorphous polyolefins used here, the magnitude of the chemical shift anisotropy was estimated from static line shape experiments to be equal to 1.5–2 kHz. From the pure polymer results in Figure 3a,c, one can extract exchange intensities $E(T)$ vs temperature for chain specific locations, i.e., backbone CH_2 vs side-group CH_3. This is an important control experiment, since it eliminates any uncertainty associated with additional side-group dynamics that might influence the interpretation of the CODEX results in the blend. Figure 4 shows systematic comparisons of CODEX exchange intensities measured from backbone CH_2 vs side-group CH_3 in the two pure polymers over the entire temperature range for which a measurable exchange signal is detected. The onset of detectable exchange intensity for either functional group, as well as the temperature of the maximum $E(T)$ value, is identical within each polymer. The absolute value of the maximum $E(T)$ is markedly different for the CH_2 vs CH_3 signals in the PEB-66 polymer, indicative of additional ethyl branch motions which

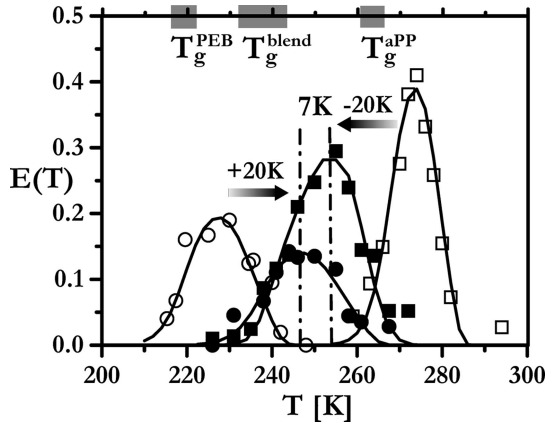

Figure 5. Normalized exchange intensities $E(T)$ for pure PEB66 (○), PEB66 in the blend (●), pure aPP (□), and aPP in the blend (■). The smooth lines are fits to the data using an Arrhenius model as described in the text. Note shifts of equal but opposite magnitude for each component upon blend formation, but a lack of complete convergence to a common temperature for the exchange intensity maximum of each polymer in the blend. The 5 K/min scan DSC T_g range for each polymer and the blend is plotted for reference on the top of the figure, with the box length representing the beginning and end of the endotherm.

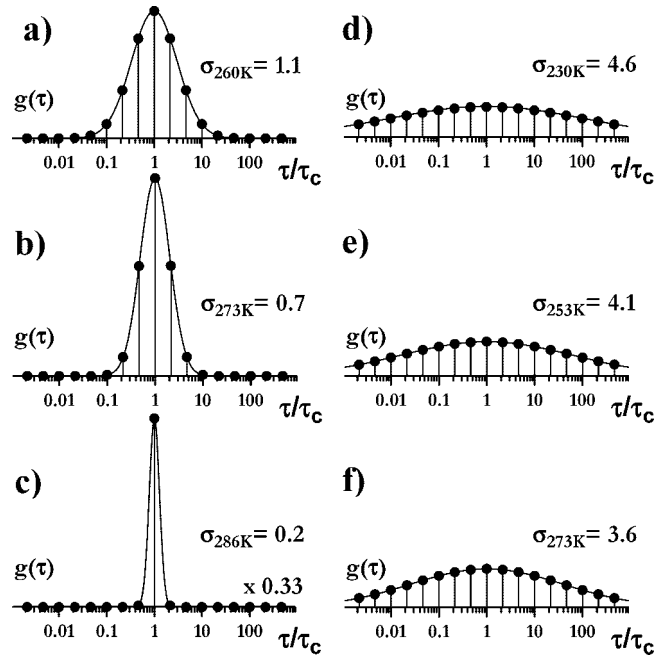

Figure 6. Discrete version of log-Gaussian correlation time distribution for aPP, with different widths σ following a linear temperature dependence $\sigma(T) = ak_BT + \sigma_0$, at key temperatures previously shown in Figure 5. Each distribution is centered at τ_c and consists of 17 points equally spaced over ~6 decades. (a) Pure aPP at 260 K, (b) pure aPP at 273 K, (c) pure aPP at 286 K, (d) aPP in blend at 230 K, (e) aPP in blend at 253 K, and (f) aPP in blend at 273 K. The $\sigma = 0.2$ distribution (c) was scaled by 0.33 to allow comparison with the other temperatures.

further reduce the magnitude of the chemical shift anisotropy for that pendant methyl group relative to backbone moieties, thereby decreasing $E(T)$ values compared to the backbone CH_2. The exchange intensity for this CH_3 group did increase in experiments with longer recoupling times (not shown), as previously demonstrated on another polyolefin blend system.[21] Since only a single carbon−carbon bond separates the CH_3 group from the main chain in aPP, this dramatic difference in exchange intensity relative to the backbone is not observed. Two important points from this control experiment are (1) the temperature of the maximum $E(T)$ value is independent of which group is measured, which means that the CH_3 signals can accurately report conformational exchange in the blend, an advantage given that they are better resolved than their respective CH or CH_2 backbone counterparts and can be deconvoluted accurately, and (2) the onset of detectable $E(T)$ signal in the CODEX experiment agrees with DSC data, in that the first one or two data points on the low-temperature side of each curve coincide with the DSC T_g (PEB66 = 219 K and aPP = 262 K).

Large changes in the temperature dependence of slow conformational exchange are observed for each pure polymer following formation of the blend, as summarized by the pure CODEX exchange intensity $E(T)$ vs temperature in Figure 5. Figure 5 represents the outcome of three independent temperature-dependent experiments: one each for the two pure polymers and a single experiment for the blend from which polymer specific exchange intensities were extracted at each temperature. Prior to any consideration of a quantitative model to fit the results, several key points may be discerned via simple inspection of the raw data in Figure 5, comparing the response of the CH_3 signal in the CODEX experiment for each pure polymer to the response of that same polymer in the blend. First, the PEB66 exchange intensity curve shifts to higher temperature in the blend relative to pure chains (PEB66 is the lower T_g component). Similarly, the exchange intensity curve shifts to lower temperature for the aPP in the blend compared to its pure response. For the PEB66, the $E(T)$ maximum shifts from 227 to 247 K upon blend formation, while the aPP $E(T)$ maximum changes from the pure value of 273 to 253 K in the blend. So, while each curve exhibits an identical 20 K change, they do not converge to an identical common value (5–7 K difference in $E(T)$ maxima), as we previously observed for the PIB/hhPP polyolefin blend.[21] While omitted from the figure in order to maintain clarity, the $E(T)$ vs T curve for the backbone CH_2 peak of aPP *in the blend* has a maximum at the same 252–253 K position as the CH_3 peak shown in Figure 5. Second, the breadth of each $E(T)$ curve increases for either component in the blend relative to the pure polymer, especially for aPP. Finally, the absolute value of $E(T)$ at each temperature across the detectable range decreases in the blend relative to the unmixed result for both polymer components. Although each temperature-dependent exchange intensity curve decreases in intensity and increases in breadth for the polymers in the blend compared to the pure polymers, the overall integrated area under the curve fits (vide infra) remains constant for each polymer, within the error of the data analysis. While the intermediate temperature values for the $E(T)$ curves are reminiscent of DSC results on blends, the ability to extract these specific details for each polymer in an amorphous mixture by simultaneous detection of the two unique $E(T)$ curves is difficult using traditional thermal analysis methods. We conclude from these points that the overall dynamic heterogeneity for both polymer chains increases in the blend, and in addition, it is also known that the CODEX exchange intensity decreases with increasing number of sites involved in the exchange process for a fixed recoupling and mixing time.[26] The details specifying exactly how the dynamic heterogeneity increases for both chains will be discussed in the following sections.

Data Analysis via Correlation Time Distribution and Arrhenius vs WLF Models. The fits to the experimental data shown in Figures 4 and 5 were obtained by combining isotropic rotational diffusion with a temperature-dependent discrete log-Gaussian correlation time distribution/Arrhenius model, as described briefly in the Experimental Section, in ref 21, and in detail in the Supporting Information. The absolute value of the exchange intensity $E(T)$ at each temperature, for a fixed recoupling and mixing time, depends on the correlation time

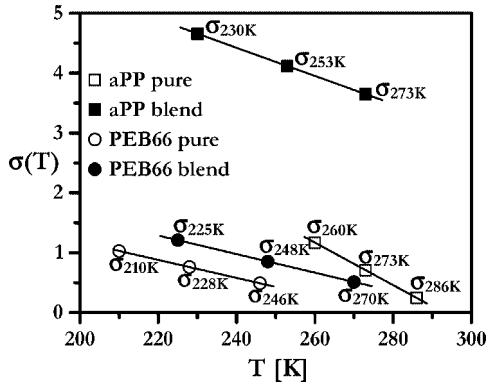

Figure 7. Temperature dependence of correlation time distribution widths for pure vs blended aPP and PEB66.

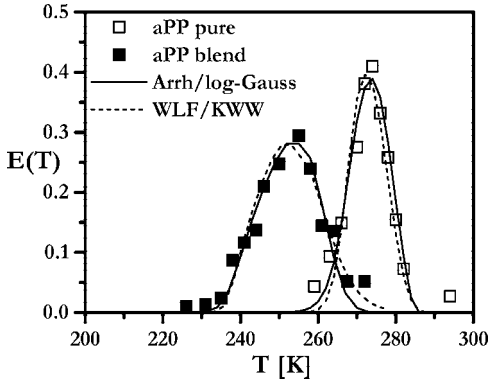

Figure 8. Comparison of fits to the aPP exchange data obtained using two different models: (1) Arrhenius temperature dependence of correlation times with variable-width log-Gaussian distribution and (2) WLF temperature dependence combined with KWW distribution. The WLF/KWW parameters for pure aPP were $C_1 = 15.5$, $C_2 = 41$ K, $\tau(T_g) = 100$ s, $T_g = 259$ K, and $\beta = 0.8$, whereas for aPP in blend $T_g = 237$ K and $\beta = 0.2$ were used.

constant characteristic of the motion modulating the chemical shift anisotropy as well as the distribution of correlation time constants for all of the segments in the amorphous polymer or polymer mixture. Figure 6 shows calculated correlation time distributions from the fits to data in Figures 4 and 5 for the aPP component, demonstrating how the $g(\tau)$ function in eq 1 can influence $E(T)$. We note how much broader the correlation time distributions become upon formation of the blend and also the increased distribution width near the T_g value (low T) for a pure polymer.

Figure 7 summarizes the temperature dependence of the correlation time distributions for both aPP and PEB66, pure and in the blend, over the entire temperature range for which an exchange signal is detected. The linear temperature dependence of $\sigma(T)$ is apparent from the figure, as is the increase in absolute value of $\sigma(T)$ for both polymers once they are in the blend. Figure 7 shows that the width of the correlation time distributions vs temperature increases much more for aPP, the high-T_g component in the blend, than that for PEB66. We recently reported a similar result for the miscible binary blend of PIB (polyisobutylene) and hhPP, where again, the hhPP (head-to-head PP) was the high T_g component and exhibited the largest perturbation in σ upon blend formation.[21]

While our primary goal is not to validate the absolute accuracy of one model versus another, but rather to understand why certain polymer chains form intimate mixtures while others do not, we do recognize that other temperature-dependent models may be more familiar to the reader. Figure 8 shows a comparison of the correlation time distribution/log-Gaussian/

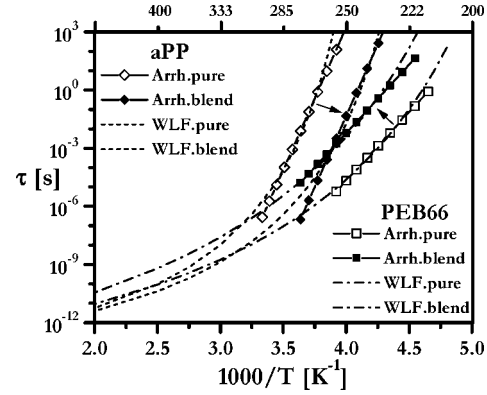

Figure 9. Temperature dependence of correlation times obtained using Arrhenius and WLF models. The WLF parameters for pure aPP were $C_1 = 15.5$, $C_2 = 41$ K, $\tau(T_g) = 100$ s, and $T_g = 259$ K, whereas for aPP in blend $T_g = 237$ K was used. For pure PEB66 we used $C_1 = 15.5$, $C_2 = 55$ K, $\tau(T_g) = 100$ s, and $T_g = 210$ K, and the best fit for PEB66 in blend was obtained with $C_2 = 68$ K and $T_g = 224$ K. An Arrhenius model can be treated as linear approximation to the WLF curve, since both Arrhenius and WLF models give similar results over the temperature range for slow motions near T_g.

Arrhenius model discussed in Figures 4−6 with a KWW/WLF analysis for the exchange intensity data from pure aPP and aPP in the blend; this is the same aPP raw data shown in Figure 5. The KWW/WLF fitting parameters are reported in the captions to Figures 8 and 9; we observe excellent agreement between the two models in terms of correlation time values over the temperature range of our data. Such low β values upon blend formation are consistent with increased dynamic heterogeneity in aPP, as recently discussed by deAzevedo using similar experiments on pure aPP,[26] and as is also readily apparent from direct inspection of the $E(T)$ exchange curve intensities in Figure 8. For convenience, comparisons of KWW β values to corresponding values of the correlation time distribution widths $g(\tau)$ are provided in the Supporting Information.

That equivalent correlation times for the center of the distribution (τ_c) are obtained using either model is more clearly evident by the representation of their temperature dependence for both polymer components in Figure 9. One observes that the temperature dependence of the slow chain dynamics for PEB66 and aPP are very different. Figure 9 also shows that while the magnitude of the change in τ_c values upon blend formation differs between the two polymers significantly at any temperature (ca. 5 decade decrease in aPP vs ca. 2.5–3 decade increase in PEB66), the two polymer components *in the blend* have identical values of τ_c near 250 K. The entire range of temperatures exhibiting equal correlation times and overlapping distributions is more evident in Figure 10, in which correlation time distributions for each polymer in the blend are shown at selected temperatures spanning the entire temperature range of interest. At the two intermediate temperatures shown in Figure 10, the two correlation time distributions completely overlap, and the central correlation time constants are essentially equal at 253 K. In total, these data indicated (1) that in a miscible polymer blend, the central correlation time constants τ_c converge to the same or nearly the same value, but (2) the widths of the correlation time distributions do not. For comparative purposes, Figure 11 shows overlapping symmetrical correlation time distributions for the PIB/hhPP blend discussed previously in ref 21, at the common temperature of the maximum value of $E(T)$ for each component in the miscible blend.

Conclusions

The data from Figures 5−10 indicate that (1) in a miscible polymer blend, the central correlation time constants τ_c converge

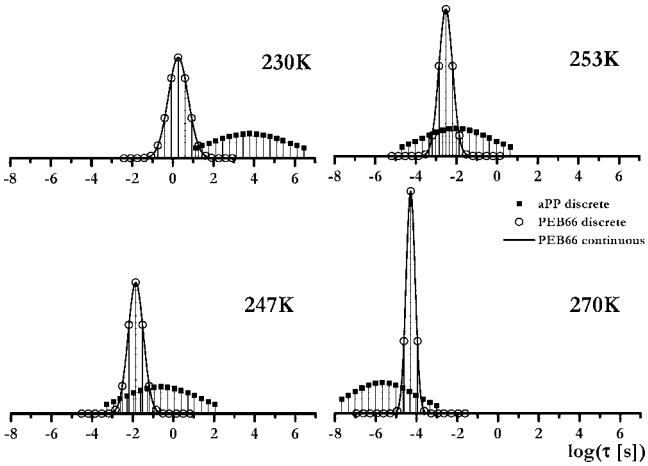

Figure 10. Correlation time distributions for aPP and PEB66 in the blend at selected temperatures spanning the range of detectable CODEX exchange intensity.

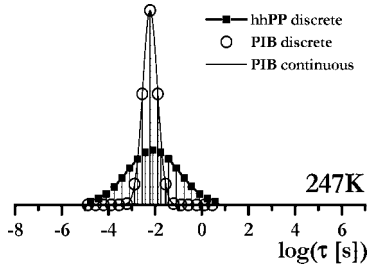

Figure 11. Correlation time distributions for individual polymer components in the miscible hhPP/PIB blend of ref 21, at the temperature of maximum exchange intensity $E(T)_{max}$, showing the same central correlation time value τ_c but largely different correlation time distribution widths σ.

to the same value, but (2) the relative widths of the correlation time distributions actually diverge dramatically (even though both do increase) compared to the pure polymer results. In addition, and in agreement with our previously published work on miscible PIB/hhPP blends (see Figure 11 and Figures 6−9 in ref 21), it is the high-T_g component that exhibits the largest change in absolute value of central correlation time constants and in the width correlation time distributions. Figures 5 and 8 show that the $E(T)$ vs T curve is the most asymmetric for the high-T_g aPP component in the blend, even though its pure component curve is symmetric about the $E(T)_{max}$ temperature value. Also, and in agreement with that previous study, the limiting values of the correlation time distribution width σ at T_g for any of the four pure amorphous polymers studied to date by this experimental approach (PIB, hhPP, aPP, and PEB66) are between 1.1 and 1.4 (see Figure 7). This value corresponds to ∼1 decade of dynamic heterogeneity in slow segmental dynamics (correlation time constants 1 ms ≤ τ_c ≤ 1000 ms) of the pure amorphous polymers.

Each of the points raised in the preceding paragraph address key questions recently raised in the literature about the dynamics of miscible polymer blends and also reveal by experiment the details of slow segmental dynamics of both pure and mixed polymers near the glass transition temperature.[12–20,33] While previous two-dimensional site-specific exchange experiments indicate that conformational trans−gauche isomerizations take place in polyolefin chains over the temperature ranges where we detect a CODEX exchange signal,[10,11] such motions cannot simply occur for two adjacent monomers, as a trans diad is longer than a gauche, for example. Since all monomers are connected in the chain, the rest of the chain and its immediate environment through space must accommodate the resulting change in length for even a single trans−gauche jump. At temperatures below T_g, such events occur with very long time constants; Figure 5 indicates that the onset of detectable numbers of these events for aPP, PEB66, and their blend occurs at essentially identical temperatures in the CODEX NMR experiment and DSC (for the specific experimental parameters used here). Although the experimental data reported here do not reveal the exact size of the rearranging regions, the quantitative values of their central correlation time constants τ_c and the temperature dependence of the correlation time distributions are in every way consistent with recent models invoking characteristic lengths of dynamic heterogeneities or cooperatively rearranging regions which increase as the temperature increases above T_g.[13,14,33] Without question, the fact that individual trans−gauche conformational exchange does occur for amorphous polyolefins indicates a minimum length scale from a purely intrachain perspective of 2–3 monomer units but does not reveal the maximum length of concerted conformational events within or among several nearby chain segments. The current view in the literature is that the characteristic length of the cooperatively rearranging regions near T_g range from 1 to 5 nm, inclusive of the Kuhn length which would be polymer-specific.[12–20] That such dynamics could be selectively interrogated via the chemical shift anisotropy for mechanically relevant polymer dynamics was described many years ago, albeit in a different experimental strategy than used here.[34]

The direct observation chain-specific CODEX experiments clearly show that, irrespective of the characteristic lengths of the cooperatively rearranging regions near T_g for either of the four polyolefins studied to date, the heterogeneity in the dynamics associated with this latent "structure" increases upon miscible blend formation. The convergence in central correlation time constants τ_c but large divergence in the correlation time distribution widths for the miscible blends is unequivocal. The degree to which recently discussed ideas regarding "self-concentration" and "concentration fluctuation" contribute to this increased heterogeneity is unclear, however; our experiments certainly are consistent with an increased "concentration fluctuation" contribution in the miscible blends.[20]

Our conclusions regarding the larger questions of why only a few polyolefin pairs form a miscible binary blend, based on these results for the aPP/PEB66 system, remain unchanged from our previous publications in which PIB was always one blend component.[10,11,21] As we have previously discussed, the increased width in the correlation time distributions in the blend, particularly for the high-T_g component, are consistent with an increased configurational entropy model and concomitant increased size of the characteristic dynamic heterogeneity near T_g relative to either of the unmixed components. Quantitatively, the change can be evaluated using the Adams−Gibbs equation[35]

$$\tau_{ex} = \tau_0 \exp(c/TS_c)$$

where we equate τ_{ex} to τ_c, the value of the correlation time at the center of the distribution at the temperature of maximum CODEX exchange intensity in the blend $(T_{em})_{blend}$. Using Figures 5 and 9, and assuming τ_0 ranging from 10^{-12} to 10^{-15} s and c as constant for each polymer in pure vs mixed state at the temperature $(T_{em})_{blend}$ = 248–253 K, we determine that the change in configurational entropy for PEB66 chains ranges from −0.81 to −0.85 upon blend formation, while the corresponding range for aPP is +1.35 to +1.28. In total for both PEB66 and aPP, $(S_c)_{blend}$ ranges from $1.16(S_c)_{unmixed}$ to $1.13(S_c)_{unmixed}$, meaning that there is approximately a 15% increase in the total configurational entropy of the miscible blend compared to the two unmixed components. We consider this a lower limit, since as applied to only the central correlation time constant, it does

not capture the large increases in correlation time distributions for both polymer components, and particularly aPP, upon formation of the miscible blend. Although their work focused on isotactic PP/PEE blends in the melt, our conclusions regarding miscibility for aPP/PEB66 qualitatively agree with those of Bates and co-workers, in which conformational asymmetry leads to excess entropies of mixing in the blend if appropriate branch concentrations exist in the PEB copolymer.[6] While our previous conclusions on entropic contributions to polyolefin miscibility were derived from experiments on polyolefin blends in which PIB was always one of the components (PIB/PEB66 and PIB/hhPP), and given that PIB has been considered an anomalous blend component, the conclusions from this study on aPP/PEB66 suggest a more widespread phenomenon for polyolefin blends specifically and for weakly interacting amorphous macromolecules in general.

Acknowledgment. The authors thank the National Science Foundation for support of this work through Grant DMR-0611474. A DuPont Science and Engineering Award (J.L.W.) provided additional research funding. Support for research instrumentation was provided by North Carolina State University and Oklahoma State University.

Supporting Information Available: Details of model calculations, fitting parameters, and comparisons to other experimental approaches. This material is available free of charge via the Internet at http://pubs.acs.org.

References and Notes

(1) Lohse, D. J.; Graessley, W. W. Thermodynamics of Polyolefin Blends. In *Polymer Blends: Formulation and Performance*; Paul, D. R., Bucknall, C. B., Eds.; Wiley: New York, 2000; Vol. *1*, Chapter 8, pp 219–237.
(2) Zhang, X.; Wang, Z.; Han, C. C. *Macromolecules* **2006**, *39*, 7441–7445.
(3) Kaminsky, W.; Hoff, M.; Derlin, S. *Macromol. Chem. Phys.* **2007**, *208*, 1341–1348.
(4) Balazs, A. C.; Emrick, T.; Russell, T. P. *Science* **2006**, *314*, 5802.
(5) Rissanou, A. N.; Peristera, L. D.; Economau, I. G. *Polymer* **2007**, *48*, 3883.
(6) Weimann, P. A.; Jones, T. D.; Hillmyer, M. A.; Bates, F. *Macromolecules* **1997**, *30*, 3650.
(7) Graessley, W. W.; Krishnamoorti, R.; Reichart, G. C.; Balsara, N. P.; Fetter, L. J.; Lohse, D. J. *Macromolecules* **1995**, *28*, 1260.
(8) Reichart, G. C.; Graessley, W. W.; Register, R. A.; Krishnamoorti, R.; Lohse, D. J. *Macromolecules* **1997**, *30*, 3036.
(9) Yamaguchi, M.; Miyata, H. *Macromolecules* **1999**, *32*, 5911.
(10) Wolak, J.; Jia, X.; Gracz, H.; Stejskal, E. O.; Wachowicz, M.; Jurga, S. J.; White, J. L. *Macromolecules* **2003**, *36*, 4844–4850.
(11) Wolak, J. E.; Jia, X.; White, J. L. *J. Am. Chem. Soc.* **2003**, *125*, 13660–13661.
(12) Lodge, T.; McLeish, T. C. B. *Macromolecules* **2000**, *33*, 5278.
(13) Cangialosi, D.; Alegria, A.; Colmonero, J. *Macromolecules* **2006**, *39*, 7149.
(14) Cangialosi, D.; Alegria, A.; Colmonero, J. *Macromolecules* **2006**, *39*, 448.
(15) Krygier, E.; Lin, G. X.; Mendes, J.; Mukandela, G.; Azar, D.; Jones, A. A.; Pathak, J. A.; Colby, R. H.; Kumar, S. K.; Floudas, G.; Krishnamoorti, R.; Faust, R. *Macromolecules* **2005**, *38*, 7721.
(16) Kant, R.; Kumar, S. K.; Colby, R. H. *Macromolecules* **2003**, *36*, 10087.
(17) Roland, C. M.; Casalini, R. *Macromolecules* **2007**, *40*, 3631.
(18) Lutz, T. R.; He, Y.; Ediger, M. D. *Macromolecules* **2005**, *38*, 9826.
(19) Lutz, T. R.; He, Y.; Ediger, M. D. *Macromolecules* **2004**, *37*, 6440.
(20) Kumar, S. K.; Shenogin, S.; Colby, R. H. *Macromolecules* **2007**, *40*, 5759.
(21) Wachowicz, M.; White, J. L. *Macromolecules* **2007**, *40*, 5433.
(22) deAzevedo, E.; Hu, W. G.; Bonagamba, T. J.; Schmidt-Rohr, K. *J. Am. Chem. Soc.* **1999**, *121*, 8411.
(23) deAzevedo, E.; Hu, W. G.; Bonagamba, T. J.; Schmidt-Rohr, K. *J. Chem. Phys.* **2000**, *112*, 8988.
(24) Graessley, W. W.; Krishnamoorti, R.; Balsara, N. P.; Fetters, L. J.; Lohse, D. J. *Macromolecules* **1994**, *27*, 3896.
(25) Krishnamoorti, R.; Graessley, W. W.; Fetters, L. J.; Garner, R. T.; Lohse, D. J. *Macromolecules* **1995**, *28*, 1252.
(26) deAzevedo, E. R.; Tozoni, J. R.; Schmidt-Rohr, K.; Bonagamba, T. J. *J. Chem. Phys.* **2005**, *122*, 154506.
(27) Luz, Z.; Tekely, P.; Reichert, D. *Prog. Nucl. Magn. Reson. Spectrosc.* **2002**, *41*, 83.
(28) Nozue, Y.; Sakurai, T.; Hozumi, H. *Macromolecules* **2007**, *40*, 273.
(29) Yamaguchi, M.; Miyata, H. *Macromolecules* **1999**, *32*, 5911.
(30) Thomann, Y.; Suhm, J.; Thomann, R.; Bar, G.; Maier, R. D.; Mulhaupt, R. *Macromolecules* **1998**, *31*, 5441.
(31) Wachowicz, M.; Wolak, J.; Gracz, H.; Stejskal, E. O.; Jurga, S.; White, J. L. *Macromolecules* **2004**, *37*, 4573–4579.
(32) Junker, F.; Veeman, W. S. *Macromolecules* **1998**, *31*, 7010.
(33) Ediger, M. D. *Annu. Rev. Phys. Chem.* **2000**, *51*, 99.
(34) Vega, A.; English, A. D. *Macromolecules* **1980**, *13*, 1635.
(35) Adam, G.; Gibbs, J. H. *J. Chem. Phys.* **1965**, *43*, 139.
(36) Donth, E.; Huth, H.; Beiner, M. *J. Phys.: Condens. Matter* **2001**, *13*, L451.

MA702795B